

---

# Additive Poisson Process: Learning Intensity of Higher-Order Interaction in Stochastic Processes

---

**Simon Luo**

The University of Sydney  
sluo4225@uni.sydney.edu.au

**Feng Zhou**

Tsinghua University  
zhoufeng6288@gmail.com

**Lamiaa Azizi**

The University of Sydney  
lamiae.azizi@sydney.edu.au

**Mahito Sugiyama**

National Institute of Informatics  
JST, PRESTO  
mahito@nii.ac.jp

## Abstract

We present the *Additive Poisson Process* (APP), a novel framework that can model the higher-order interaction effects of the intensity functions in stochastic processes using lower dimensional projections. Our model combines the techniques in *information geometry* to model higher-order interactions on a statistical manifold and in *generalized additive models* to use lower-dimensional projections to overcome the effects from the curse of dimensionality. Our approach solves a convex optimization problem by minimizing the KL divergence from a sample distribution in lower dimensional projections to the distribution modeled by an intensity function in the stochastic process. Our empirical results show that our model is able to use samples observed in the lower dimensional space to estimate the higher-order intensity function with extremely sparse observations.

## 1 Introduction

Consider two stochastic processes which are correlated with arrival times for an event. For a given time interval, what is the probability of observing an event from both of the stochastic processes? Can we learn the joint intensity function by just using the observations from the individual processes? Our proposed model, the *Additive Poisson Process* (APP), provides a novel solution to this problem.

The Poisson process is a counting process used in a wide range of disciplines such as time-space sequence data including transportation (Zhou et al., 2018), finance (Ilalan, 2016), ecology (Thompson, 1955), and violent crime (Taddy, 2010) to model the arrival times for a single system by learning an intensity function. When the intensity function is multiplied by a time interval, it gives the probability of a point being excited at a given time. Despite the recent advances of modeling of the Poisson processes and its wide applicability, majority of the point processes model only a single stochastic process and do not consider the correlation between two or more stochastic processes. Several models have been proposed to include events from different stochastic processes. One example is the marked Poisson process (MPP) (Baccelli et al., 2010), where the different events are marked so that a particular subset of events can be used to generate the intensity function. However, this approach has never been applied to learning of the joint intensity function but instead it identifies different events to compute the intensity function.

Another approach is kernel density estimation (KDE) (Rosenblatt, 1956), which can be used directly to learn the intensity function. However, KDE suffers from the curse of dimensionality, which means that KDE requires a large size sample or a high intensity function to build an accurate model.

In addition, the complexity of the model expands exponentially with respect to the number of dimensions, which makes it infeasible to compute. Bayesian approaches such as using a mixture of beta distributions with a Dirichlet prior (Kottas, 2006) and Reproducing Kernel Hilbert Space (RKHS) (Flaxman et al., 2017) have been proposed to quantify the uncertainty by having a prior for the intensity function. However, these approaches are often non-convex, making it difficult to obtain the global optimal solution. In addition, if observation is sparse, it is hard for these approaches to learn a reasonable intensity function.

All previous models are unable to efficiently and accurately learn the intensity of the interaction between stochastic processes. This is why the intensity of the joint process is often low, leading to sparse samples or, in an extreme case, no observations at all, making it difficult to learn the intensity function from the joint samples. In this paper, we propose a novel framework to learn the higher-order interaction effects of intensity functions in stochastic processes. Our model combines the techniques introduced by Luo and Sugiyama (2019) to model higher-order interactions between stochastic processes and by Friedman and Stuetzle (1981) in *generalized additive models* to learn the intensity function using samples in a lower dimensional space.

We first show the connection between generalized additive models and Poisson processes. We then provide the connection between generalized additive models and the *log-linear model* (Agresti, 2012), which has a well-established theoretical background in information geometry (Amari, 2016). We draw parallels between the formulation of the generalized additive models and the binary log-linear model on a partially ordered set (poset) (Sugiyama et al., 2017). The learning process in our model is formulated as a convex optimization problem to arrive at a unique optimal solution using natural gradient, which minimizes the Kullback-Leibler (KL) divergence from the sample distribution in a lower dimensional space to the distribution modeled by the learned intensity function. This connection provides remarkable properties to our model: the ability to learn higher-order intensity functions using lower dimensional projections, thanks to the *Kolmogorov-Arnold representation theorem*. This property makes it advantageous to use our proposed approach for the cases where there are, no observations, missing samples, or low event rate. Our model is flexible because it can capture interaction between processes as a partial order structure in the log-linear model and the parameters of the model is fully customizable to meet the requirements for the application. Our empirical results show that our model effectively uses samples projected onto a lower dimensional space to estimate the higher-order intensity function. Our model is also robust to various sample sizes.

## 2 Formulation

In this section we first introduce the technical background in the Poisson process and its extension to a multi-dimensional Poisson process. We then introduce the Generalized Additive Model (GAM) and its connection to the Poisson process. This is followed by presenting our novel framework, called Additive Poisson Process (APP), which is our main technical contribution and has a tight link to the Poisson process modelled by GAMs. We show that learning of APP can be achieved via convex optimization using natural gradient.

### 2.1 Poisson Process

The Poisson process is characterized by an arrival intensity  $\lambda: \mathbb{R} \rightarrow \mathbb{R}$ . An inhomogeneous Poisson process is a general type of processes, where the arrival intensity changes with time. The process with time-changing intensity  $\lambda(t)$  is defined as a counting process  $\mathbb{N}(t)$ , which has an independent increment property. For all time  $t \geq 0$  and changes in time  $\delta \geq 0$ , the probability  $p$  for the observations is given as

$$\begin{aligned} p(\mathbb{N}(t + \delta) - \mathbb{N}(t) = 0) &= 1 - \delta\lambda(t) + o(\delta) \\ p(\mathbb{N}(t + \delta) - \mathbb{N}(t) = 1) &= \delta\lambda(t) + o(\delta) \\ p(\mathbb{N}(t + \delta) - \mathbb{N}(t) \geq 2) &= o(\delta) \end{aligned}$$

where  $o(\cdot)$  denotes little-o notation (Daley and Vere-Jones, 2007). Given a realization of timestamps  $\{\mathbf{t}_i\}_{i=1}^N \subseteq [0, T]^D$  from an inhomogeneous (multi-dimensional) Poisson process with intensity  $\lambda$ , where we assume multiple processes and  $\text{dom}(\lambda) = \mathbb{R}^D$ . Each  $\mathbf{t}_i \in \mathbb{R}^D$  is the time of occurrence for

the  $i$ -th event across  $D$  processes and  $T$  is the observation duration. The likelihood for the Poisson process (Daley and Vere-Jones, 2007) is given by

$$p\left(\{\mathbf{t}_i\}_{i=1}^N \mid \lambda(\mathbf{t})\right) = \exp\left[-\int \lambda(\mathbf{t}) d\mathbf{t}\right] \prod_{i=1}^N \lambda(\mathbf{t}_i), \quad (1)$$

where  $\mathbf{t} = [t^{(1)}, \dots, t^{(D)}] \in \mathbb{R}^D$ . We define the functional prior on  $\lambda(\mathbf{t})$  as

$$\lambda(\mathbf{t}) := g[f(\mathbf{t})] = \exp[f(\mathbf{t})]. \quad (2)$$

The function  $g(\cdot)$  is a positive function to guarantee the non-negativity of intensity which we choose to be the exponential function, and our objective is to learn the function  $f(\cdot)$ . The log-likelihood of the multi-dimensional Poisson process with the functional prior is described as

$$\log p\left(\{\mathbf{t}_i\}_{i=1}^N \mid \lambda(\mathbf{t})\right) = \sum_{i=1}^N f(\mathbf{t}_i) - \int \exp[f(\mathbf{t})] d\mathbf{t}. \quad (3)$$

In the following sections, we introduce *generalized additive models* and the *information geometric formulation of the log-linear model* to learn  $f(\mathbf{t})$  and the normalizing term.

## 2.2 Generalized Additive Model

In this section we outline our finding: the connection between Poisson processes with Generalized Additive Model (GAM) proposed by Friedman and Stuetzle (1981). GAM projects higher-dimensional features into lower-dimensional space to apply smoothing functions to build a restricted class of non-parametric regression models. GAM is less affected by the curse of dimensionality compared to directly using smoothing in a higher-dimensional space. For a given set of processes  $J \subseteq [D] = \{1, \dots, D\}$ , the traditional GAM using one-dimensional projections is defined as

$$\log \lambda_J(\mathbf{t}) = \sum_{j \in J} f_j(t^{(j)}) - \beta_J,$$

with some smoothing function  $f_j$ .

In this paper, we extend it to include higher-order interactions between features in GAM. The  $k$ -th order GAM is defined as

$$\begin{aligned} \log \lambda_J(\mathbf{t}) &= \sum_{j \in J} f_{\{j\}}(t^{(j)}) + \sum_{j_1, j_2 \in J} f_{\{j_1, j_2\}}(t^{(j_1)}, t^{(j_2)}) + \dots + \sum_{j_1, \dots, j_k \in J} f_{\{j_1, \dots, j_k\}}(t^{(j_1)}, \dots, t^{(j_k)}) - \beta_J \\ &= \sum_{I \subseteq J, |I| \leq k} f_I(\mathbf{t}^{(I)}) - \beta_J, \end{aligned} \quad (4)$$

where  $\mathbf{t}^{(I)} \in \mathbb{R}^{|I|}$  denotes the subvector  $(\mathbf{t}^{(j)})_{j \in I}$  of  $\mathbf{t}$  with respect to  $I \subseteq [D]$ . The function  $f_I : \mathbb{R}^{|I|} \rightarrow \mathbb{R}$  is a smoothing function to fit the data, and the normalization constant  $\beta_J$  for the intensity function is obtained as

$$\beta_J = \int \lambda_J(\mathbf{t}) d\mathbf{t} = \int \exp\left[\sum_{J' \subseteq J} f_{J'}(\mathbf{t}^{(J')})\right] d\mathbf{t}. \quad (5)$$

The definition of the additive model is in the same form as Equation (2). In particular, if we compare Equation (2) and (4), we can see that the smoothing function  $f$  in (2) corresponds to the right-hand side of (4).

Learning a continuous function using lower dimensional projections is well known because of the *Kolmogorov-Arnold representation theorem*, which states as follows:

**Theorem 1** (Kolmogorov–Arnold Representation Theorem (Braun and Griebel, 2009; Kolmogorov, 1957)). *Any multivariate continuous function can be represented as a superposition of one-dimensional functions, i.e.,*

$$f(t_1, \dots, t_n) = \sum_{q=1}^{2n+1} f_q \left[ \sum_{p=1}^n g_{q,p}(t) \right]. \quad (6)$$

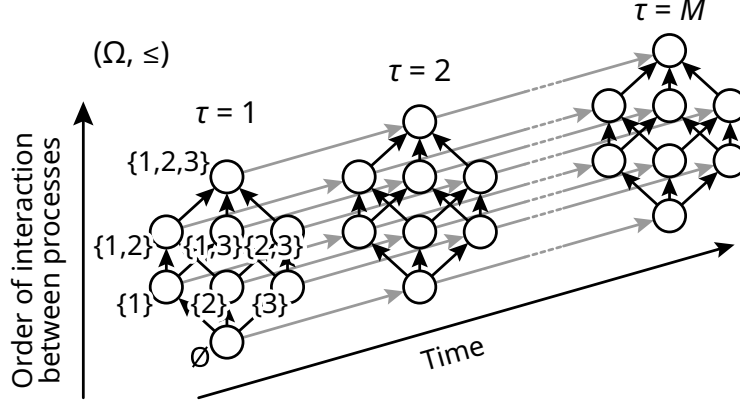


Figure 1: Partial order structured sample space  $(\Omega, \leq)$  with  $D = 3$ .

Braun (2009) showed that the GAM is an approximation to the general form presented in Kolmogorov-Arnold representation theorem by replacing the range  $q \in \{1, \dots, 2n + 1\}$  with  $I \subseteq J$  and the inner function  $f_{q,p}$  by the identity if  $q = p$  and zero otherwise, yielding  $f(\mathbf{t}) = \sum_{I \subseteq J} f_I(\mathbf{t}^{(I)})$ .

Interestingly, the canonical form for additive models in Equation (4) can be rearranged to be in the same form as Kolmogorov-Arnold representation theorem. By letting  $f(\mathbf{t}) = \sum_{I \subseteq J} f_I(\mathbf{t}^{(I)}) = g^{-1}(\lambda(\mathbf{t}))$  and  $g(\cdot) = \exp(\cdot)$ , we have

$$\lambda_J(\mathbf{t}) = \frac{1}{\exp(\beta_J)} \exp \left[ \sum_{I \subseteq J} f_I(\mathbf{t}^{(I)}) \right] \propto \exp \left[ \sum_{I \subseteq J} f_I(\mathbf{t}^{(I)}) \right], \quad (7)$$

where we assume  $f_I(\mathbf{t}^{(I)}) = 0$  if  $|I| > k$  for the  $k$ -th order model and  $1/\exp(\beta_J)$  is the normalization term for the intensity function. Based on the Kolmogorov-Arnold representation theorem, generalized additive models is able to learn the intensity of the higher-order interaction between stochastic processes by using projections into lower dimensional space. In the next section we draw parallels between using higher-order interactions studied in *information geometry* and the lower dimensional projections in *generalized additive models*.

### 2.3 Additive Poisson Process

We introduce our key technical contribution in this section, the information geometric formulation of the *additive Poisson process*. In the following, we discretize the time window  $[0, T]$  into  $M$  bins and treat each bin as a natural number  $\tau \in [M] = \{1, 2, \dots, M\}$  for each process. We assume that  $M$  is predetermined by the user. First we introduce a structured space for the Poisson process to incorporate interactions between processes. Let  $\Omega = \{ (J, \tau) \mid J \in 2^{[D]}, \tau \in [M] \}$ . We define the *partial order* (Davey and Priestley, 2002) on  $\Omega$  as

$$(J, \tau) \leq (J', \tau') \text{ if } J \subseteq J' \text{ and } \tau \leq \tau', \quad \text{for each } \omega = (J, \tau), \omega' = (J', \tau') \in \Omega, \quad (8)$$

which is illustrated in Figure 1. The relation  $J \subseteq J'$  is used to model any-order interactions between stochastic processes (Luo and Sugiyama, 2019) (Amari, 2016, Section 6.8.4) and each  $\tau$  in  $(J, \tau)$  represents “time” in our model. Note that the domain of  $\tau$  can be generalized from  $[M]$  to  $[M]^D$  to take different time stamps into account, while in the following we assume that observed time stamps are always the same across processes for simplicity. Our experiments in the next section demonstrates that we can still accurately estimate the density of processes. Our model can be applied to not only time-series data but any sequential data.

On any set equipped with a partial order, we can introduce a *log-linear model* (Sugiyama et al., 2016, 2017). Given a parameter domain  $\mathcal{S} \subseteq \Omega$ . For a partially ordered set  $(\Omega, \leq)$ , the log-linear model with parameters  $(\theta(s))_{s \in \mathcal{S}}$  is introduced as

$$\log p(\omega; \theta) = \sum_{s \in \mathcal{S}, s \leq \omega} \theta(s) - \psi(\theta) \quad (9)$$

---

**Algorithm 1** Additive Poisson Process (APP)
 

---

- 1: **Function** APP( $\{\mathbf{t}_i\}_{i=1}^N, \mathcal{S}, M, h$ ):
  - 2: Initialize  $\Omega$  with the number  $M$  of bins
  - 3: Apply Gaussian Kernel with bandwidth  $h$  on  $\{\mathbf{t}_i\}_{i=1}^N$  to compute  $\hat{p}$
  - 4: Compute  $\hat{\eta} = (\hat{\eta}(s))_{s \in \mathcal{S}}$  from  $\hat{p}$
  - 5: Initialize  $\boldsymbol{\theta} = (\theta(s))_{s \in \mathcal{S}}$  (randomly or  $\theta(s) = 0$ )
  - 6: **repeat**
  - 7:   Compute  $p$  using the current  $\boldsymbol{\theta} = (\theta(s))_{s \in \mathcal{S}}$
  - 8:   Compute  $\boldsymbol{\eta} = (\eta(s))_{s \in \mathcal{S}}$  from  $p$
  - 9:    $\Delta\boldsymbol{\eta} \leftarrow \boldsymbol{\eta} - \hat{\boldsymbol{\eta}}$
  - 10:   Compute the Fisher information matrix  $\mathbf{G}$  using Equation (12)
  - 11:    $\boldsymbol{\theta} \leftarrow \boldsymbol{\theta} - \mathbf{G}^{-1}\Delta\boldsymbol{\theta}$
  - 12: **until** convergence of  $\boldsymbol{\theta} = (\theta(s))_{s \in \mathcal{S}}$
  - 13: **End Function**
- 

for each  $\omega \in \Omega$ , where  $\psi(\theta) \in \mathbb{R}$  is the partition function uniquely obtained as

$$\psi(\theta) = \log \sum_{\omega \in \Omega} \exp \left[ \sum_{s \in \mathcal{S}, s \leq \omega} \theta(s) \right] = -\theta(\perp)$$

and  $\perp \in \Omega$  is the least element of  $\Omega$ ; that is,  $\perp \leq \omega$  for all  $\omega \in \Omega$ . A special case of this formulation coincides with the density function of the *Boltzmann machines* (Sugiyama et al., 2018; Luo and Sugiyama, 2019). The remarkable property is that we can re-write it in the form of Kolmogorov-Arnold representation theorem as

$$p(\omega; \theta) = \frac{1}{\exp \psi(\theta)} \exp \left[ \sum_{s \in \mathcal{S}, s \leq \omega} \theta(s) \right] \propto \exp \left[ \sum_{s \in \mathcal{S}, s \leq \omega} \theta(s) \right], \quad (10)$$

which is the same formulation with Equation (7) from an information geometric perspective. Therefore, the intensity  $\lambda$  of the multi-dimensional Poisson process given via the GAM in Equation (7) is fully modeled (parameterized) by Equation (9) and each intensity  $f_I(\cdot)$  is obtained as  $\theta((I, \cdot))$ .

We use the above log-linear model to formulate the additive Poisson process on our partially ordered sample space  $\Omega$  defined in Equation (8). To consider the  $k$ -th order model, we consistently use the parameter domain  $\mathcal{S}$  given as

$$\mathcal{S} = \{(J, \tau) \in \Omega \mid |J| \leq k\},$$

where  $k$  is an input parameter to the model that specifies the upper bound of the order of interactions. This means that  $\theta(s) = 0$  for all  $s \notin \mathcal{S}$ . Note that our model is well-defined for any subset  $\mathcal{S} \subseteq \Omega$  and the user can use arbitrary domain in applications.

For a given  $J$  and each bin  $\tau$  with  $\omega = (J, \tau)$ , the empirical probability  $\hat{p}(\omega)$  is given as

$$\hat{p}(\omega) = \frac{1}{Z} \sum_{I \subseteq J} \sigma_I(\tau), \quad Z = \sum_{\omega \in \Omega} \hat{p}(\omega), \quad \text{and } \sigma_I(\tau) := \frac{1}{Nh_I} \sum_{i=1}^N K \left[ \frac{\tau^{(I)} - \mathbf{t}_i^{(I)}}{h_I} \right], \quad (11)$$

for each discretized state  $\omega = (J, \tau)$ , where  $\boldsymbol{\tau} = (\tau, \dots, \tau) \in \mathbb{R}^D$ . The function  $\sigma_I$  performs smoothing on time stamps  $\{\mathbf{t}_i\}_{i=1}^N$ , which is the kernel smoother proposed by Buja et al. (1989). The function  $K$  is a kernel and  $h_I$  is the bandwidth for each projection  $I \subseteq [D]$ . We use the Gaussian kernel as  $K$  to ensure that probability is always nonzero, meaning that the definition of the kernel smoother coincides with the kernel estimator of the intensity function proposed by Schäbe (1993).

## 2.4 Optimization

Given an empirical distribution  $\hat{p}$  defined in Equation (11), the task is to learn the parameter  $(\theta(s))_{s \in \mathcal{S}}$  such that the distribution via the log-linear model in Equation (9) is close to  $\hat{p}$  as much as possible. Let us define  $\mathfrak{S}_{\mathcal{S}} = \{p \mid \theta(s) = 0 \text{ if } s \notin \mathcal{S}\}$ , which is the set of distributions that can be represented by the log-linear model using the parameter domain  $\mathcal{S}$ . Then the task is formulated as  $\min_{p \in \mathfrak{S}_{\mathcal{S}}} D_{\text{KL}}(\hat{p}, p)$ , where  $D_{\text{KL}}(\hat{p}, p) = \sum_{\omega \in \Omega} \hat{p} \log(\hat{p}/p)$  is the KL divergence from  $\hat{p}$  to  $p$ . It is known that this problem can be solved by *e-projection*, which coincides with the maximum likelihood

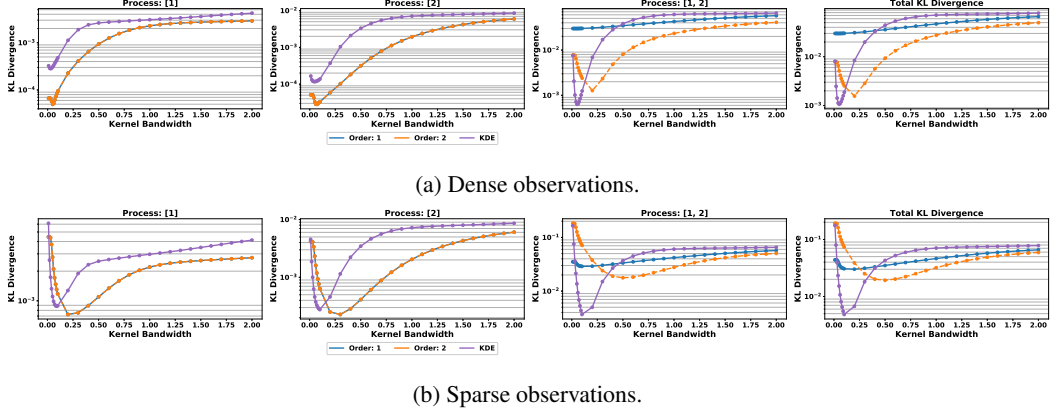


Figure 2: KL Divergence for four-order Poisson process.

estimation, and it is always convex optimization (Amari, 2016, Chapter 2.8.3). The gradient with respect to each parameter  $\theta(s)$  is obtained by

$$\frac{\partial}{\partial \theta(s)} D_{\text{KL}}(\hat{p}, p) = \eta(s) - \hat{\eta}(s), \quad \text{where } \eta(s) = \sum_{\omega \geq s} p(\omega).$$

The value  $\eta(s)$  is known as the expectation parameter (Sugiyama et al., 2017) and  $\hat{\eta}(s)$  is obtained by replacing  $p$  with  $\hat{p}$  in the above equation. If  $\hat{\eta}(s) = 0$  for some  $s \in \mathcal{S}$ , we remove  $s$  from  $\mathcal{S}$  to ensure that the model is well-defined.

Moreover, let the parameter domain  $\mathcal{S} = \{s_1, \dots, s_{|\mathcal{S}|}\}$  and  $\boldsymbol{\theta} = [\theta(s_1), \dots, \theta(s_{|\mathcal{S}|})]^T$ ,  $\boldsymbol{\eta} = [\eta(s_1), \dots, \eta(s_{|\mathcal{S}|})]^T$ . We can always use the *natural gradient* (Amari, 1998) as the closed form solution of the Fisher information matrix is always available (Sugiyama et al., 2017). The update step is,

$$\boldsymbol{\theta}_{\text{next}} = \boldsymbol{\theta} - \mathbf{G}^{-1}(\boldsymbol{\eta} - \hat{\boldsymbol{\eta}}),$$

where the Fisher information matrix  $\mathbf{G}$  is obtained as

$$g_{ij} = \frac{\partial}{\partial \theta(s_i) \theta(s_j)} D_{\text{KL}}(\hat{p}, p) = \sum_{\omega \geq s_i, \omega \geq s_j} p(\omega) - \eta(s_i) \eta(s_j). \quad (12)$$

Theoretically the Fisher information matrix is numerically stable to perform a matrix inversion. However, computationally floating point errors may cause the matrix to become indefinite. To overcome this issue, a small positive value is added along the main diagonal of the matrix. This technique is known as jitter and it is used in areas like Gaussian processes to ensure that the covariance matrix is computationally positive semi-definite (Neal, 1999).

The pseudocode for APP is shown in Algorithm 1. The time complexity of computing line 7 is  $\mathcal{O}(|\Omega||\mathcal{S}|)$ . This means when implementing the model using gradient descent, the time complexity of the model is  $\mathcal{O}(|\Omega||\mathcal{S}|^2)$  to update the parameters in  $\mathcal{S}$  for each iteration. For natural gradient the cost of inverting the Fisher information matrix  $G$  is  $\mathcal{O}(|\mathcal{S}|^3)$ , therefore the time complexity to update the parameters in  $\mathcal{S}$  is  $\mathcal{O}(|\mathcal{S}|^3 + |\Omega||\mathcal{S}|)$  for each iteration. The time complexity for natural gradient is significantly higher to invert the fisher information matrix, if the number of parameter is small, it is more efficient to use natural gradient because it requires significantly less iterations. However, if the number of parameters is large, it is more efficient to use gradient descent.

### 3 Experiments

We perform experiments using two dimensional synthetic data, higher dimensional synthetic data, and rea-world data to evaluate the performance of our proposed approach. Our code is implemented on Python 3.7.5 with NumPy version 1.8.2 and the experiments are run on Ubuntu 18.04 LTS with an Intel i7-8700 6c/12t with 16GB of memory. In experiments of synthetic data, we simulate random

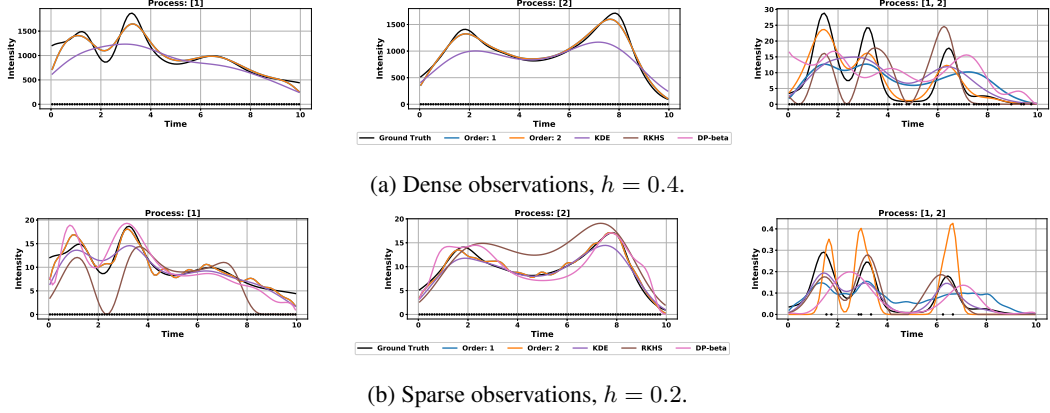


Figure 3: Intensity function of two dimensional processes. Dots represent observations.

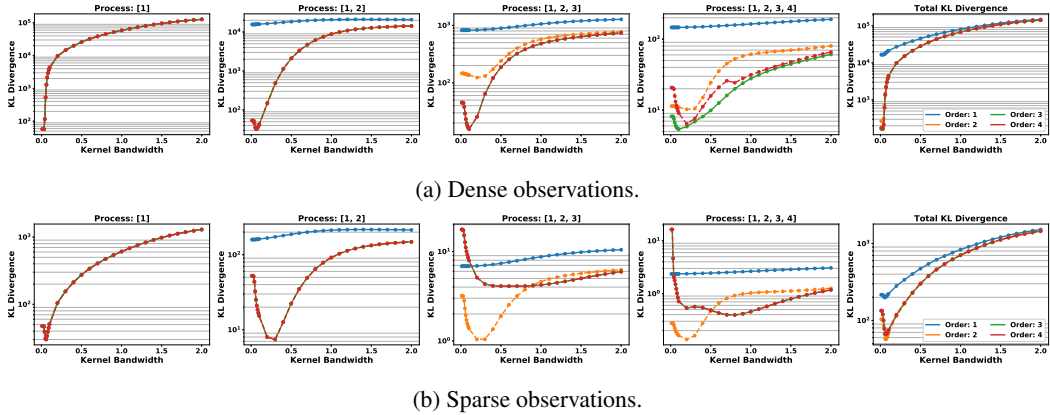


Figure 4: KL Divergence for four-order Poisson process.

events using Equation (1). We generate an intensity function using a mixture of Gaussians, where the mean is drawn from a uniform distribution and the covariance is drawn from an inverted Wishart distribution. The intensity function is then the density function multiplied by the sample size. The synthetic data is generated by directly drawing a sample from the probability density function with the predetermined sample size. The sample size is randomly chosen by the mixture of Gaussians. We then run our models and compare with Kernel Density Estimation (KDE) (Rosenblatt, 1956), an inhomogeneous Poisson process whose intensity is estimated by a reproducing kernel Hilbert space formulation (RKHS) (Flaxman et al., 2017), and a Dirichlet process mixture of Beta distributions (DP-beta) (Kottas, 2006). The hyper-parameters  $M$  and  $h$  in our proposed model are selected using grid search and cross-validation. For situations where a validation set is not available, then  $h$  could be selected using a rule of thumb approach such as Scott’s Rule (Scott, 2015) and  $M$  could be selected empirically from the input data by computing the time interval of the joint observation.

### 3.1 Experiments on Two-Dimensional Processes

For our experiment, we use 20 Gaussian components and simulate a dense case with 100,000 observations and a sparse case with 1,000 observations within the time frame of 10 seconds. We consider that a joint event occurs if the two events occur 0.1 seconds apart. Figure 2a and Figure 2b compares the KL divergence between the first- and second-order models. In the first-order processes, both first- and second-order models have the same performance. This is expected as both of the model can treat first-order interactions and is able to learn the empirical intensity function exactly which is the superposition of the one-dimensional projection of the Gaussian kernels on each observation. For the second-order process, the second-order model performs better than the first-order model because it is able to directly learn the intensity function from the projection onto the two-dimensional space.

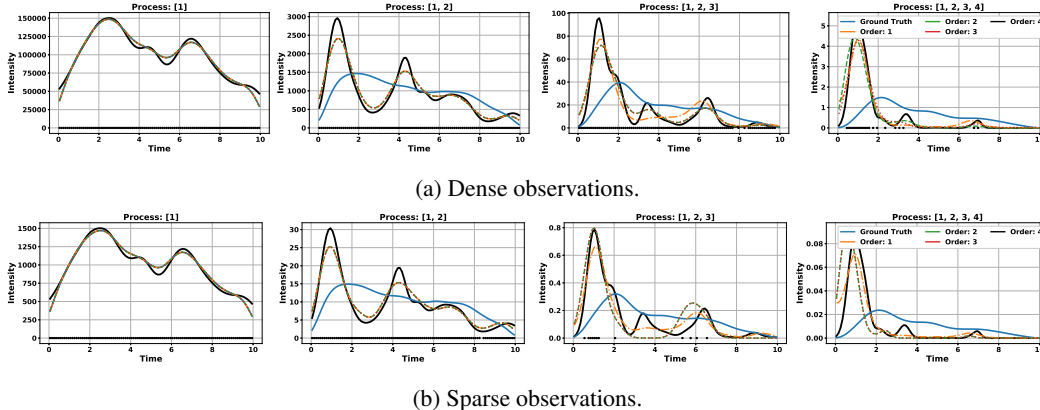


Figure 5: Intensity function of higher dimensional processes. Dots represent observations.

Table 1: The lowest KL divergence from the ground truth distribution to the obtained distribution on two types of single processes ([1] and [2]) and joint process of them ([1,2]). APP-# represents the order of the Additive Poisson Process. Missing values mean that the computation did not finish within two days.

	Process	APP-1	APP-2	KDE	RKHS	DP-beta
Dense	[1]	<b>4.98e-5</b>	<b>4.98e-5</b>	2.81e-4	-	-
	[2]	<b>2.83e-5</b>	<b>2.83e-5</b>	1.17e-4	-	-
	[1,2]	2.98e-2	1.27e-3	<b>6.33e-4</b>	4.09e-2	4.54e-2
Sparse	[1]	<b>7.26e-4</b>	<b>7.26e-4</b>	8.83e-4	1.96e-2	2.62e-3
	[2]	<b>2.28e-4</b>	<b>2.28e-4</b>	2.76e-4	2.35e-3	2.49e-3
	[1,2]	2.88e-2	1.77e-2	<b>3.67e-3</b>	1.84e-2	3.68e-2

In contrast, the first-order model must approximate the second-order process using the observations from the first order-processes. In the sparse case, the second-order model performs better when the correct bandwidth is selected.

Table 1 compares our approach with other state-of-the-art approaches. Our proposed approach, APP, performs the best for first-order processes in both the sparse and dense experiments. The experiments for RKHS and DP-beta were unable to complete running within 2 days for the dense experiment. In the second-order process our approach was outperformed by KDE, while both the second-order APP is able to outperform both RKHS and DP-beta process for both sparse and dense experiments. Figure 2a and Figure 2b shows that KDE is sensitive to changes in bandwidth, which means that, for any practical implementation of the model, second-order APP with a less sensitive bandwidth is more likely to learn a more accurate intensity function when the ground truth is unknown.

### 3.2 Experiments on Higher-Dimensional Processes

We generate a fourth-order process to simulate the behaviour of the model in higher dimensions. The model is generalizable to higher dimensions, however it is difficult to demonstrate results for processes higher than fourth-order. For our experiment, we generate an intensity function using 50 Gaussian components and draw a sample with the size of  $10^7$  for the dense case and that with the size of  $10^5$  for the sparse case. We consider the joint event to be the time frame of 0.1 seconds.

We were not able to run comparison experiments with other models because they are unable to learn when there are no or few direct observations in third- and fourth-order processes. In addition, the time complexity is too high to learn from direct observations in first- and second-order processes because all the other models have their time complexity proportional to the number of observations. The time complexity for KDE is  $\mathcal{O}(N^D)$  for the dimensionality with  $D$ , while DP-beta is  $\mathcal{O}(N^2K)$ , where  $K$  is the number of clusters, and RKHS is  $\mathcal{O}(N^2)$  for each iteration with respect to the sample size  $N$ , where DP-beta and RKHS are applied to a single dimension as they cannot directly treat

Table 2: Negative test log-likelihood for the New York Taxi data. Single processes ([T] and [W]) and joint process of them ([T,W]). APP-# represents the order of the Additive Poisson Process.

	Process	APP-1	APP-2	KDE	RKHS	DP-beta
Jan	[T]	714.07	714.07	<b>713.77</b>	728.13	731.01
	[W]	745.60	745.60	<b>745.23</b>	853.42	790.04
	[T,W]	249.60	<b>246.05</b>	380.22	259.29	260.30
Feb	[T]	<b>713.43</b>	<b>713.43</b>	755.71	908.52	765.76
	[W]	<b>738.66</b>	<b>738.66</b>	773.65	1031.00	792.10
	[T,W]	328.84	<b>244.21</b>	307.86	348.96	326.52
Mar	[T]	<b>716.72</b>	<b>716.72</b>	733.74	755.48	741.28
	[W]	<b>738.06</b>	<b>738.06</b>	816.99	853.33	832.43
	[T,W]	291.20	<b>246.19</b>	289.69	328.47	300.36

multiple dimensions. KDE is able to make an estimation of the intensity function when there are no direct observations, however, it was too computationally expensive to complete running the experiment. Differently, our model is more efficient because the time complexity is proportional to the number of bins in our model. The time complexity of APP for each iteration is  $\mathcal{O}(|\Omega||\mathcal{S}|)$ , where  $|\Omega| = M^D$  and  $|\mathcal{S}| = \sum_{c=1}^k \binom{D}{c}$ . Our model scales combinatorially with respect to the number of dimensions. However, this is unavoidable for any model which directly takes into account the high-order interactions. For practical applications, the number of dimensions  $D$  and the order of the model  $k$  is often small, making it feasible to compute.

In Figure 4a we observe similar behaviour in the model, where the first-order processes fit precisely to the empirical distribution generated by the Gaussian kernels. The third-order model is able to period better on the fourth-order process. This is because the observation shown in Figure 5a is largely sparse and learning from the observations directly may overfit. A lower dimensional approximation is able to provide a better result in the third-order model. Similar trends can be seen in the sparse case as shown in Figure 4b, where a second-order model is able to produce better estimation in third- and fourth-order processes. The observations are extremely sparse as seen in Figure 5b, where there are only a few observations or no observations at all to learn the intensity function.

### 3.3 Uncovering Common Patterns in the New York Taxi Dataset

We demonstrate the capability of our model on the 2016 Green Taxi Trip dataset<sup>1</sup>. We are interested in finding the common pick up patterns across Tuesday and Wednesday. We define a common pick up time to be within 1 minute intervals of each other between the two days. We have chosen to learn an intensity function using the Poisson process for Tuesday and Wednesday and a joint process for both of them. The joint process uncovers the common pick up patterns between the two days. We have selected to use the first two weeks of Tuesday and Wednesday in January 2016 as our training and validation sets and Tuesday and Wednesday of the third week of January 2016 as our testing set. We repeat the same experiment for February and March.

We show our results in Table 2, where we use the negative test log-likelihood as a evaluation measure. APP-2 has consistently outperformed all the other approaches for the joint process between Tuesday and Wednesday. In addition, for the individual process, APP-1 and -2 also showed the best result for February and March. These results also demonstrate the effectiveness of our model in capturing the higher-order interactions between processes, which is difficult for the other existing approaches.

## 4 Conclusion

We have proposed a novel framework, called *Additive Poisson Process* (APP), to learn the intensity function of the higher-order interaction between stochastic processes using samples from lower dimensional projections. We formulated our proposed model using the *the binary log-linear model* and optimize it using information geometric structure of the parameter space. We drew parallels

<sup>1</sup><https://data.cityofnewyork.us/Transportation/2016-Green-Taxi-Trip-Data/hvrh-b6bn>

between our proposed model and *generalized additive model* and the ability to learn from lower dimensional projections via the *Kolmogorov-Arnold representation theorem*. Our empirical results show the superiority of our method when learning the higher-order interactions between stochastic processes when there are no direct observations or are extremely sparse. Our model also has superior run-time compared to other approaches making the model much more efficient and robust to varying sample sizes. Our approach provides a novel formulation to learn the joint intensity function which typically has extremely low intensity. There is enormous potential to apply them to real-world applications, where higher order interaction effects need to be model such as in transportation, finance, ecology, and violent crimes.

## References

- Alan Agresti. *Categorical Data Analysis*. Wiley, 3 edition, 2012.
- Shun-Ichi Amari. Natural gradient works efficiently in learning. *Neural Computation*, 10(2):251–276, 1998.
- Sun-Ichi Amari. *Information Geometry and Its Applications*. Springer, 2016.
- François Baccelli, Bartłomiej Błaszczyszyn, et al. Stochastic geometry and wireless networks: Volume II applications. *Foundations and Trends in Networking*, 4(1–2):1–312, 2010.
- Jürgen Braun. *An application of Kolmogorov’s superposition theorem to function reconstruction in higher dimensions*. PhD thesis, Universitäts-und Landesbibliothek Bonn, 2009.
- Jürgen Braun and Michael Griebel. On a constructive proof of Kolmogorov’s superposition theorem. *Constructive Approximation*, 30(3):653, 2009.
- Andreas Buja, Trevor Hastie, and Robert Tibshirani. Linear smoothers and additive models. *The Annals of Statistics*, 17(2):453–510, 1989.
- Daryl J Daley and David Vere-Jones. *An Introduction to the Theory of Point Processes: Volume II: General Theory and Structure*. Springer, 2007.
- Brian A Davey and Hilary A Priestley. *Introduction to Lattices and Order*. Cambridge University Press, 2002.
- Seth Flaxman, Yee Whye Teh, and Dino Sejdinovic. Poisson intensity estimation with reproducing kernels. *Electronic Journal of Statistics*, 11(2):5081–5104, 2017.
- Jerome H Friedman and Werner Stuetzle. Projection pursuit regression. *Journal of the American Statistical Association*, 76(376):817–823, 1981.
- Deniz Ilalan. A poisson process with random intensity for modeling financial stability. *The Spanish Review of Financial Economics*, 14(2):43–50, 2016.
- Andrei Nikolaevich Kolmogorov. On the representation of continuous functions of many variables by superposition of continuous functions of one variable and addition. In *Doklady Akademii Nauk*, volume 114, pages 953–956. Russian Academy of Sciences, 1957.
- Athanasios Kottas. Dirichlet process mixtures of beta distributions, with applications to density and intensity estimation. In *Workshop on Learning with Nonparametric Bayesian Methods, 23rd International Conference on Machine Learning (ICML)*, volume 47, 2006.
- Simon Luo and Mahito Sugiyama. Bias-variance trade-off in hierarchical probabilistic models using higher-order feature interactions. In *Proceedings of the 33rd AAAI Conference on Artificial Intelligence*, volume 33, pages 4488–4495, 2019.
- Radford M Neal. Regression and classification using gaussian process priors. *Bayesian Statistics*, 6: 475–501, 1999.
- Yosihiko Ogata. On Lewis’ simulation method for point processes. *IEEE Transactions on Information Theory*, 27(1):23–31, 1981.

- Murray Rosenblatt. Remarks on some nonparametric estimates of a density function. *The Annals of Mathematical Statistics*, pages 832–837, 1956.
- H Schäbe. Nonparametric estimation of intensities of nonhomogeneous poisson processes. *Statistical Papers*, 34(1):113–131, 1993.
- David W Scott. *Multivariate density estimation: theory, practice, and visualization*. John Wiley & Sons, 2015.
- Mahito Sugiyama, Hiroyuki Nakahara, and Koji Tsuda. Information decomposition on structured space. In *2016 IEEE International Symposium on Information Theory*, pages 575–579, 2016.
- Mahito Sugiyama, Hiroyuki Nakahara, and Koji Tsuda. Tensor balancing on statistical manifold. In *Proceedings of the 34th International Conference on Machine Learning*, volume 70 of *Proceedings of Machine Learning Research*, pages 3270–3279, 2017.
- Mahito Sugiyama, Hiroyuki Nakahara, and Koji Tsuda. Legendre decomposition for tensors. In *Advances in Neural Information Processing Systems 31*, pages 8825–8835, 2018.
- Matthew A Taddy. Autoregressive mixture models for dynamic spatial poisson processes: Application to tracking intensity of violent crime. *Journal of the American Statistical Association*, 105(492): 1403–1417, 2010.
- HR Thompson. Spatial point processes, with applications to ecology. *Biometrika*, 42(1/2):102–115, 1955.
- Feng Zhou, Zhidong Li, Xuhui Fan, Yang Wang, Arcot Sowmya, and Fang Chen. A refined MISD algorithm based on Gaussian process regression. In *Pacific-Asia Conference on Knowledge Discovery and Data Mining*, pages 584–596. Springer, 2018.

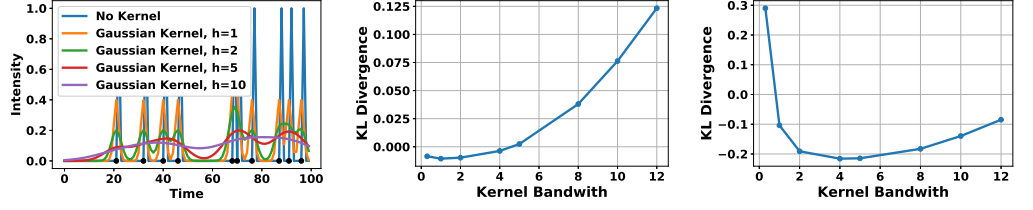
## A Additional Experiments

### A.1 Bandwidth Sensitivity Analysis

Our first experiment is to demonstrate the ability for our proposed model to learn an intensity function from samples. We generate a Bernoulli process with probably of  $p = 0.1$  to generate samples for every 1 seconds for 100 seconds to create a toy problem for our model. This experiment is to observe the behaviour of varying the bandwidth in our model. In Figure 6a, we observe that applying no kernel, we learn the deltas of each individual observation. When we apply a Gaussian kernel, the output of the model for the intensity function is much more smooth. Increasing the bandwidth of the kernel will provide a wider and much smoother function. Between the 60 seconds and 80 seconds mark, it can be seen when two observations have overlapping kernels, the intensity function becomes larger in magnitude.

### A.2 One Dimensional Poisson Process

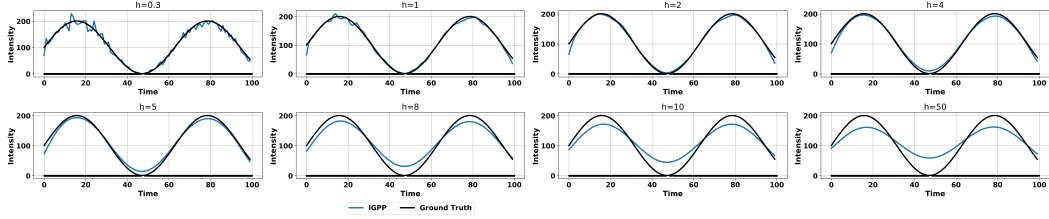
A one dimensional experiment is simulated using Ogata’s thinning algorithm (Ogata, 1981). We generate two experiments use the standard sinusoidal benchmark intensity function with a frequency of  $20\pi$ . The dense experiment has troughs with 0 intensity and peaks at 201 and the sparse experiment has troughs with 0 intensity and peaks at 2. Figure 6d shows the experimental results of the dense case, our model has no problem learning the intensity function. We compare our results using KL divergence between the underlying intensity function used to generate the samples to the intensity function generated by the model. Figure 6b shows that the optimal bandwidth is  $h = 1$ .



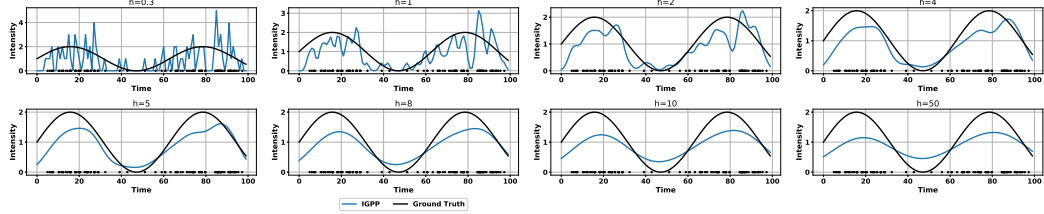
(a) Toy Example

(b) KL divergence of dense experiment

(c) KL divergence of sparse experiment



(d) Ogata's thinning algorithm with high intensity



(e) Ogata's thinning algorithm with low intensity

Figure 6: One dimensional experiments

---

**Algorithm 2** Thinning Algorithm for non-homogenous Poisson Process

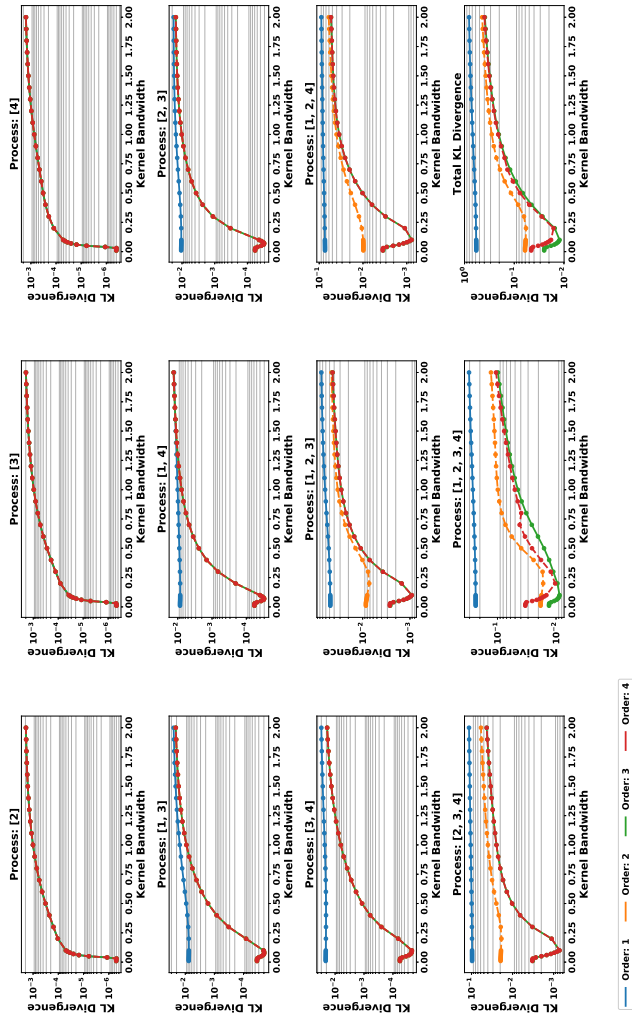
---

```

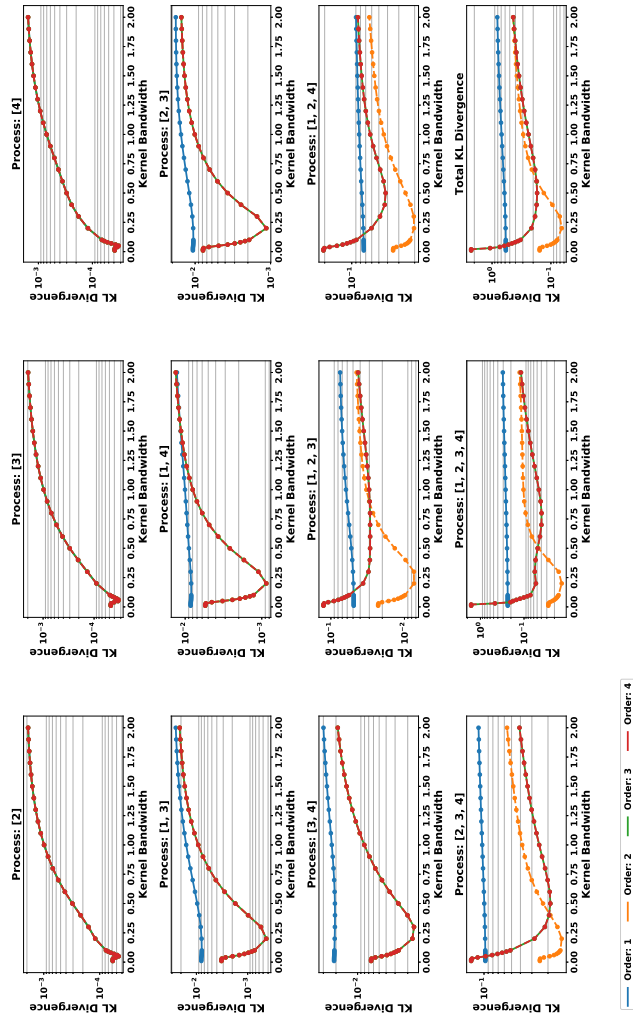
1: Function Thinning Algorithm ( $\lambda(t), T$ ):
2:  $n = m = 0, t_0 = s_0 = 0, \bar{\lambda} = \sup_{0 \leq t \leq T} \lambda(t)$ 
3: repeat
4:    $u \sim \text{uniform}(0, 1)$ 
5:    $w = -\frac{1}{\bar{\lambda}} \ln u \{w \sim \text{exponential}(\bar{\lambda})\}$ 
6:    $s_{m+1} = s_m + w$ 
7:    $D \sim \text{uniform}(0, 1)$ 
8:   if  $D \leq \frac{\lambda(s_{m+1})}{\bar{\lambda}}$  then
9:      $t_{n+1} = s_{m+1}$ 
10:     $n = n + 1$ 
11:  else
12:     $m = m + 1$ 
13:  end if
14:  if  $t_n \leq T$  then
15:    return  $\{t_k\}_{k=1,2,\dots,n}$ 
16:  else
17:    return  $\{t_k\}_{k=1,2,\dots,n-1}$ 
18:  end if
19: until  $s_m \leq T$ 
20: End Function

```

---



(a) Dense observations.



(b) Sparse observations.

Figure 7: KL Divergence for four-order Poisson process.

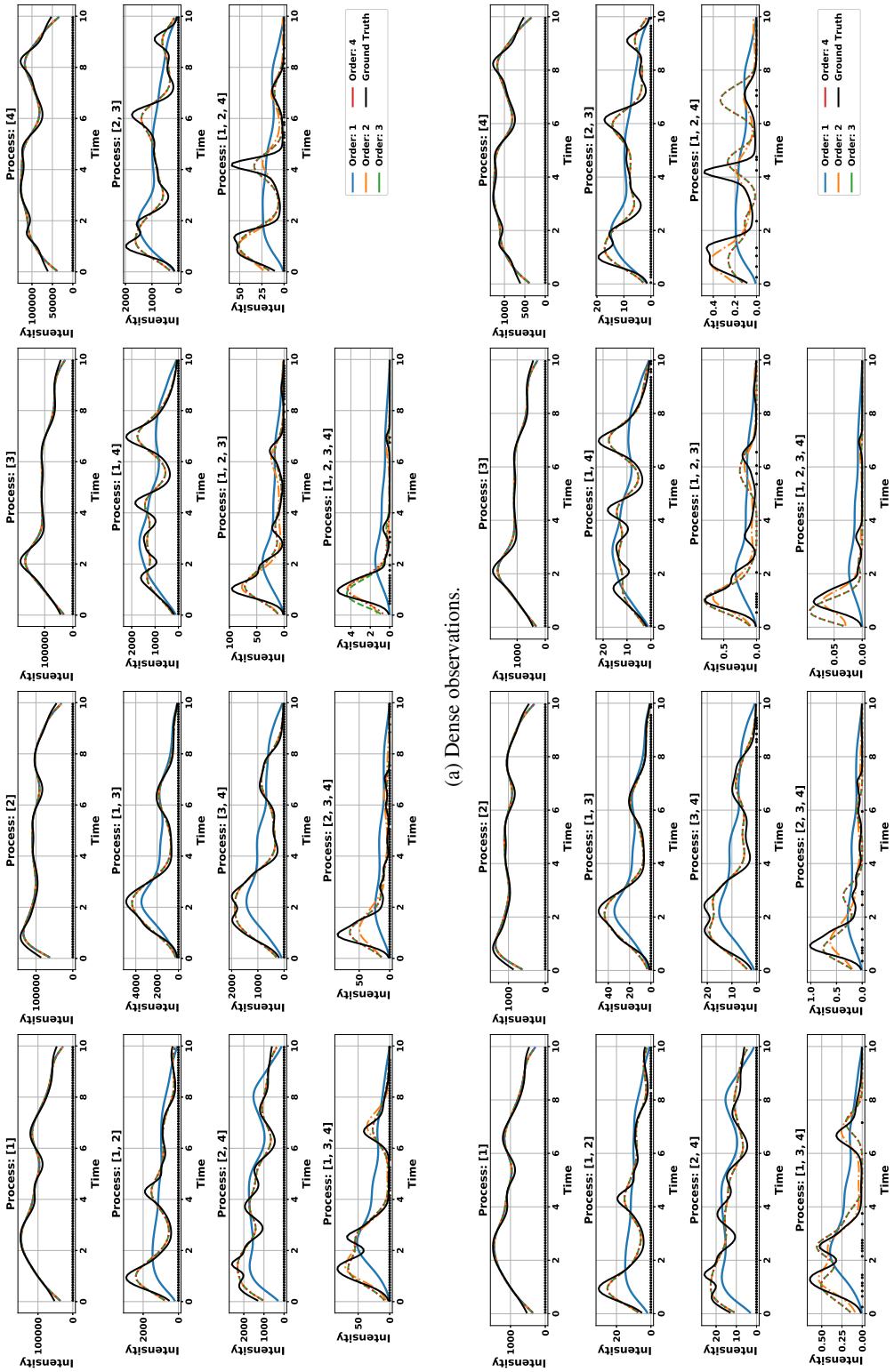


Figure 8: Intensity function of higher dimensional processes. Dots represent observations.